JOURNAL OF OPTOELECTRONICS AND ADVANCED MATERIALS Vol. 9, No. 12, December 2007, p. 3843 - 3846

On low concentration aqueous magnetic fluid light scattering properties

D. CHICEA*, M. RĂCUCIU
"Lucian Blaga" University, Faculty of Science, Dr. I. Ratiu Street, No.5-7, 550024, Sibiu, Romania

Nanostructured Fe_3O_4 particles were prepared by co-precipitation of acidic solutions of Fe (II) and Fe (III). The aggregation of the particles was prevented by using a 25% solution of tetramethylammonium hydroxide as surfactant. The TEM analysis revealed an average size of the ferrofluid particles of 7.7 nm. An experiment consisting of a He-Ne laser source, a cuvette, a frame grabber and a computer was set up investigate the light scattering properties of aqueous magnetic fluid in the very small concentration range. Digital movies of the far field interference having magnetic fluid at different concentrations as target were recorded and analyzed using a computer code written for this purpose. For each movie the averages of the intensity, contrast and speckle size were calculated. The variation of these parameters with the magnetic fluid concentration was found and plotted. We found that the average intensity, contrast and speckle size have a smooth and slow variation with the magnetic fluid concentration except for a specific region where the variation is stronger. The procedure can be used further on to measure the volume ratio in the 0 – 500 ppm concentration range, which otherwise is difficult to be measured using other techniques.

(Received November 11, 2007; accepted December 4, 2007)

Keywords: Magnetic fluid, Light scattering, Speckle analysis, Very low concentration measurement

1. Introduction

The synthesis of magnetite (Fe_3O_4) nanoparticles has been of interest for long, because of they have many technological applications especially in the form of magnetic fluids. A magnetic fluid also known as a ferrofluid is a suspension of nanosize ferromagnetic or ferrimagnetic particles in a carrier liquid (polar and non-polar solvents). Magnetic fluids (ferrofluids) represent a well defined category of magnetically controllable nanomaterials with fluid properties. Fe_3O_4 magnetite nanoparticles can be produced by mixing Fe(II) and Fe(III) salts together in a basic solution. Colloidal stability is assured by coating the particles with nonmagnetic molecular surfactants shell that prevents close approach of the magnetic nanoparticles thereby reducing the possibility of aggregation via van der Waals forces or magnetic attractions [1].

The ferrofluids are convenient for simulating and studying disordered systems, because their structure and particles concentration can easily be controlled by adjusting the synthesis procedure parameters [2].

Dynamic and static light scattering experiments became important tools for the investigation and characterization of structural and dynamic properties of complex fluids, e.g. colloids [3].

Due to their big particle density, the ferrofluids are opaque to visible light [4]. In order to investigate the light scattering properties, the ferrofluid particle concentration must be small.

When coherent light crosses a medium having scattering centers an un-uniformly illuminated image is obtained, currently named speckled image, having a statistical distribution of the intensity over the interference field. The speckled image appears as a result of the interference of the wavelets scattered by the scattering centers, each wavelet having a different phase and amplitude in each location of the interference field. The image changes in time as a consequence of the scattering centers (SC hereafter) complex movement of sedimentation and Brownian motion. This produces fluctuations of the image intensity in each location of the interference field. These fluctuations give the aspect of "boiling speckles" [5], [6].

The speckled image can be observed either in free space and is named objective speckle or on the image plane of a diffuse object illuminated by a coherent source; it is named subjective speckle in [5]. The review paper [6] classifies the two types of speckled images as far field speckle and image speckle. In this work the objective speckle, respectively far field speckle is considered.

Dynamical speckle analysis has become a current method to characterize the dynamic behavior of scattering medium such as flow, sediment and Brownian movement. The motion of the speckle field was analyzed by correlometric methods [7, 8, 9] or by laser speckle contrast analysis [10, 11]. The speckle size can be used to measure the roughness of a surfaces [12, 13, 14] or to determinate the thickness of semi-transparent thin slab like in [15]. Most of the above mentioned experiments use the backscattered light speckle configuration. In papers like [16] a different optical set-up is used to measure the correlation function in the near field, and show the near-field speckle dependence on the particles size. The work reported in [17, 18] uses a transmission optical set-up to measure the far field parameters like contrast and speckle size. The transmission type of setup was used in the work.

The next sections present details of the ferrofluid synthesis, the optical experimental setup and the results of the far field interference pattern analysis.

2. Experimental

2.1 Ferrofluid synthesis and physical properties

The water-based magnetic fluid used in this study was synthetised in our laboratory by co-precipitation method, at room temperature. Fe_3O_4 nanoparticles were prepared by co-precipitation method of acidic solutions of Fe (II) and Fe (III) in according with [19] modified by [20]. The aggregation of the particles was prevented by using a 25% solution of tetramethylammonium hydroxide as surfactant. The ferrofluid batch synthesized in our laboratory was dark brown, exhibited positive magnetic behavior in the presence of a permanent magnet, and kept their colloidal characteristics for up to 12 months. Low level of magnetic fluid nanoparticles sedimentation in time was observed. The particles have been characterized using a TESLA transmission electron microscope. The analysis of all TEM pictures revealed a mean physical diameter about 7.7 nm of the particles. The saturation magnetization of the initial magnetic fluid sample was 9800 A/m. The density of magnetic fluid sample was measured using a picnometric method at temperature of 295K and was found to be about 1059kg/m^3. Viscosity measurements were carried out by capillary method using an Ubbelohde viscosimeter and we found that the dynamic viscosity was 2.02×10^{-3} kg/ms value for the initial magnetic fluid sample.

2.2 Experimental setup and data processing procedure

A transmission type of experiment was of set-up. The schematic is presented in Fig. 1. The He-Ne laser had a wavelength of 632 nm and a constant power of 2 mW. The active area of the glass cuvette was 12 mm thick. Measurements were done at 3.5 degrees from the beam axis using a CMOS camera and data acquisition was done on a PC using the USB port. The optical system of the camera was removed, therefore the recorded images are the direct interference on the CMOS detection matrix. Consequently the far field speckle was recorded, not the speckle image.

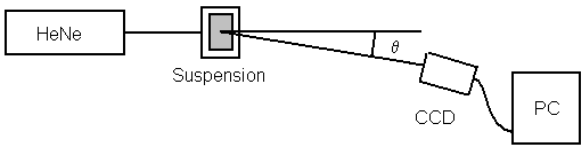

Fig. 1. The schematic of the experiment.

A typical record of the far field speckle is presented in Fig. 2.

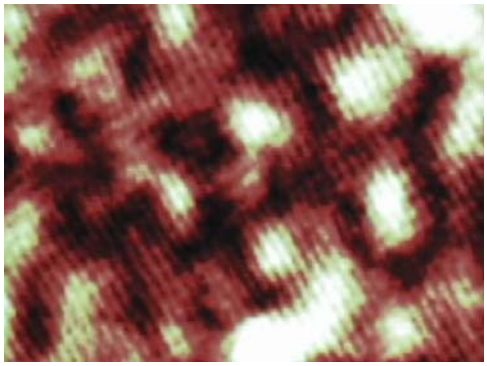

Fig. 2. A far field speckle.

The average contrast of the image, either acquired as a bitmap or extracted from the frames of the movie, is calculated [5], [17], [18] as:

$$C = \frac{\sqrt{< \left(I(i,j) - < I >\right)^2 >}}{< I >} \tag{1}$$

where $I(i,j)=I(x_i, y_j)$ is the intensity recorded by the cell (i,j) of the CCD, hence by the pixel (i,j) of the array of pixels the image consists of. This is a space contrast and not a time contrast, as described in [21]. In (1) the angular brackets stand for average over the entire 640x480 collection of intensity values for an image that is processes.

In [4], [17] and [18] the average speckle size is defined as the normalized autocovariance function of the intensity:

$$Sps = \frac{R_i(x,y) - \left\langle I(x,y)\right\rangle^2}{\left\langle I(x,y)^2\right\rangle - \left\langle I(x,y)\right\rangle^2} \tag{2}$$

where $R_i(x,y) = \left\langle I(x_i, y_i)\cdot I(0,0)\right\rangle$

In this paper a different approach is proposed to calculate the speckle size. For each vertical profile of a frame the normalized autocorrelation function [22] is calculated.

The autocorrelation function for each sample was calculated as:

$$A_n(s) = \frac{\left\langle I(n,j) * I(n,j+s)\right\rangle}{\left\langle I(n,j) * I(n,j)\right\rangle} \tag{3}$$

where the angle brackets denote averages over the coordinate y, n represents the number of the vertical profile and s is the autocorrelation distance.

The speckle size for n-th profile is defined as the value of the s (pixel number or distance, if multiplied by the pixel size on the CMOS) where the autocorrelation function decreases to 1/e. An average is calculated for each image and we define the speckle size as the average speckle size for that particular image. A vertical profile is presented in Fig. 3 and the autocorrelation function of that profile in Fig. 4.

3. Results and discussions

In the first part of the experiment a bitmap image, having a resolution of 640×480 pixels was recorded for different dilutions. Using a program written for this purpose the average intensity over the recorded area, the average contrast and the average speckle size, in pixels, were calculated. Examining the results we notice a big spread of the data in a small concentration range. This suggests that big differences between pictures taken for the same sample at different moments might occur, due to fluctuations.

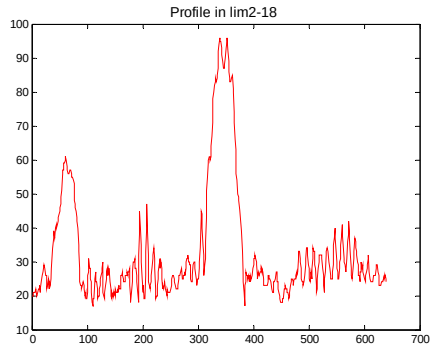

Fig. 3. A vertical intensity profile.

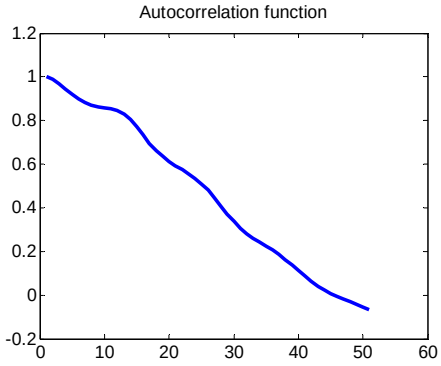

Fig. 4. The normalized autocorrelation function.

In order to verify this hypothesis, the experiment was repeated and an uncompressed, 24 bits AVI type movie was recorded for each concentration, using a framerate of 1 per second and the same resolution, 640×480 pixels. A previous experiment using a data acquisition system revealed that the autocorrelation time for this type of samples is around 0.1 – 0.3 seconds therefore a framerate of 1 per second ensures that the images in consecutive frames are not correlated and that the average over the 120 frames for each sample does not depend on the specific time they were recorded at.

Fig. 5 presents the variation of the average intensity, Figure 6 the variation of the average contrast and Figure 7 the variation of the average speckle size with the concentration. The error bars on the plots are the confidence intervals calculated using the Student test, for 120 samples (frames) for each sample and a 99% confidence level, using:

$$l = \frac{t \cdot S}{\sqrt{n}} \tag{4}$$

where t is the parameter of the Student test, S is the dispersion and n is the number of frames, 120 for this experiment.

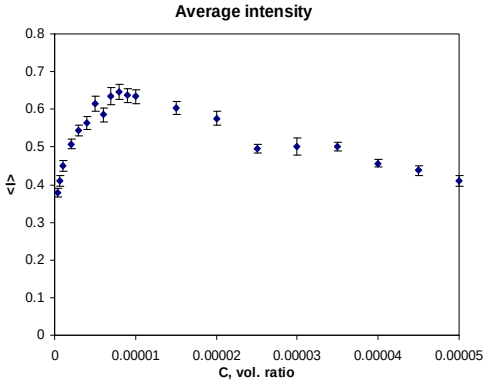

Fig. 5. The average intensity variation with the ferrofluid concentration.

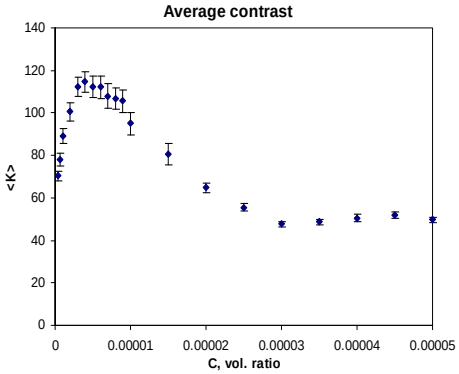

Fig. 6. The average contrast variation with the concentration.

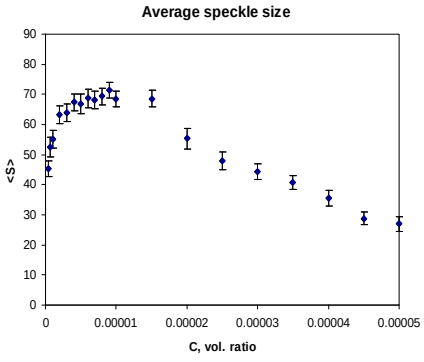

Fig. 7. The average speckle size variation with the concentration.

Examining Fig. 5 we notice that at very small ferrofluid concentration the average intensity increases with the nanoparticles concentration, presents a maximum at $9.0*10^{-6}$ and then decreases with the concentration. As the concentration increases in the range where multiple scattering is dominant, the average intensity remains constant.

The average contrast, presented in Fig. 6, has a very fast increase with the SC concentration, a maximum at 5.0×10^{-6} followed by a fast decrease. When the concentration increases the slope decreases in module and finally the concentration remains constant, as presented in Fig. 6. This variation is similar with the work reported in [17], where organic SCs were used.

The average speckle displays the same variation pattern, with a maximum at 9.0×10^{-6}, as presented in Fig. 7. The trend in these results is similar with the results reported in [17]. What appears to be very interesting is the particular linear decrease over a relatively wide concentration range.

4. Conclusions

This paper presents the results of our investigation on the light scattering properties of diluted ferrofluid nanoparticles. We found that the alternative speckle size calculation algorithm we used calculates the average speckle size in a correct manner. They also reveal that the average speckle contrast, light intensity and speckle size have a fast increase with the SC increase in the very small concentration, that is $0 - 9.\times10^{-6}$ volume ratio followed by a slow decrease in the range 10^{-6}-5.0×10^{-4} volume ratio. This trend of the curves can be used in measuring the ferrofluid nanoparticles concentration, in the extremely small concentration range, that is $0 - 9.0\times10^{-6}$. Moreover, the liner part of the average contrast can be used to measure the particle concentration in the $10^{-6} - 5.0\times10^{-4}$ volume ratio range, together with an alternative method that can indicate that the concentration is bigger than 9.0×10^{-6}.

References

[1] R. E. Rosensweig, Ferrohydrodynamics, Cambridge University Press, Cambridge (1985).
[2] E. Blums, A. Cebers, M. M. Maiorov, Magnetic liquids, de Gruytes, Ed. Berlin (1997).
[3] R. Pecora, Dynamic Light Scattering, Plenum Press, New York (1985).
[4] V. Socoliuc, D. Bica, Progr. Colloid Polym. Sci. **117**, 131 (2001).
[5] J. W. Goodman, "Statistical Properties of Laser Speckle Patterns," in Laser speckle and related phenomena, Vol.9 in series Topics in Applied Physics, J. C. Dainty, Ed., Springer-Verlag, Berlin, Heidelberg, New York, Tokyo, (1984).
[6] J. David Briers, Physiol. Meas. **22**, R35–R66 (2001).
[7] D. A. Boas, A. G. Yodh, J. Opt. Soc. Am. A **14**, 192-215 (1997).
[8] Y. Aizu, T. Asakura, Opt. Las. Tech. **23**, 205-219 (1991).
[9] I. V. Fedosov, V.V. Tuchin, Proc. of SPIE **4434**, 192-196 (2001).
[10] J. D. Briers, G. Richards, X. W. He, J. Biomed. Opt. **4**, 164-175 (1999).
[11] D. A. Zimnyakov, J. D. Briers, V. V. Tuchin, Chap. 18 in Handbook of biomedical diagnostics, Valery V. Tuchin, Ed. SPIE press, Bellingham (2002).
[12] P. Lehmann, Appl. Opt. **38**, 1144-1152 (1999).
[13] G. Da Costa, J. Ferrari, Appl. Opt. **36**, 5231-5237 (1997).
[14] R. Berlasso, F. Perez Quintian, M. A. Rebollo, C. A. Raffo, N. G. Gaggioli, Appl. Opt. **39**, 5811-5819 (2000).
[15] A. Sadhwani, K. T. Schomaker, G. J. Tearney, N. S. Nishioka, Appl. Opt. **35**, 5727-5735 (1996).
[16] M. Giglio, M. Carpineti, A. Vailati, D. Brogioli, Appl. Opt. **40**, 4036-4040 (2001).
[17] Y. Piederrière, J. Cariou, Y. Guern, B. Le Jeune, G. Le Brun, J. Lotrian, Optics Express. **12**(1), 176-188 (2004).
[18] Y. Piederriere, J. Le Meur, J. Cariou, J. F. Abgrall, M. T. Blouch, Optics Express **12**(19), 4596 – 4601 (2004).
[19] S. Palacin, P.C. Hidber, J. Bourgoin, C. Miramond, C. Fermon, G. Whitesides, Chem. Mater. **8**, 1316 (1996).
[20] J. Breitzer, G. Lisensky, J. Chem. Educ. **76**, 943 (1999).
[21] R. Nothdurft, G. Yao, Optics Express **13**(25), 10034 – 10039 (2005).
[22] R. Bracewell, The Fourier Transform and Its Applications, 3rd ed. New York: McGraw-Hill, pp. 40-45 (1999).

*Corresponding author: dan.chicea@ulbsibiu.ro